THE JOURNAL OF BIOLOGICAL CHEMISTRY
Vol. 277, No. 31, Issue of August 2, pp. 28330–28339, 2002
Printed in U.S.A.

Disabling Receptor Ensembles with Rationally Designed Interface Peptidomimetics*

Received for publication, March 25, 2002, and in revised form, April 24, 2002
Published, JBC Papers in Press, May 14, 2002, DOI 10.1074/jbc.M202880200

Alan Berezov, Jinqiu Chen, Qingdu Liu, Hong-Tao Zhang, Mark I. Greene‡, and Ramachandran Murali§

From the Department of Pathology and Laboratory Medicine, University of Pennsylvania School of Medicine and the Abramson Family Cancer Research Institute, Philadelphia, Pennsylvania 19104

Members of the erbB family receptor tyrosine kinases (erbB1, erbB2, erbB3, and erbB4) are overexpressed in a variety of human cancers and represent important targets for the structure-based drug design. Homo- and heterodimerization (oligomerization) of the erbB receptors are known to be critical events for receptor signaling. To block receptor self-associations, we have designed a series of peptides derived from potential dimerization surfaces in the extracellular subdomain IV of the erbB receptors (erbB peptides). In surface plasmon resonance (BIAcore) studies, the designed peptides have been shown to selectively bind to the erbB receptor ectodomains and isolated subdomain IV of erbB2 with submicromolar affinities and to inhibit heregulin-induced interactions of erbB3 with different erbB receptors. A dose-dependent inhibition of native erbB receptor dimerization by the erbB peptides has been observed in 32D cell lines transfected with different combinations of erbB receptors. The peptides effectively inhibited growth of two types of transformed cells overexpressing different erbB receptors, T6-17 and 32D, in standard MTT (3-(4,5-dimethylthiazol-2-yl)-2,5-diphenyltetrazolium bromide) and cell viability assays. The study identifies distinct loops within the membrane-proximal part of the subdomain IV as potential receptor-receptor interaction sites for the erbB receptors and demonstrates the possibility of disabling receptor activity by structure-based targeting of the dimerization interfaces. Molecular models for possible arrangement of the erbB1·EGF complex, consistent with the involvement of subdomain IV in inter-receptor interactions, are proposed. Small dimerization inhibitors described herein can be useful as probes to elucidate different erbB signaling pathways and may be developed as therapeutic agents.

erbB2 (neu, HER2) is a member of the epidermal growth factor or HER family of tyrosine kinase receptors that also includes erbB1 (EGFR,[1] HER1), erbB3 (HER3), and erbB4 (HER4) (1–4). Overexpression of erbB receptors has been found in many types of human cancer raising the possibility that receptor-directed therapies may be useful as cancer management strategies. Greater expression of erbB2 on transformed cells than on normal epithelial tissues allows selective targeting of tumor cells using various approaches (5–13). A variety of strategies have also been developed for targeting the erbB1 receptor, including monoclonal antibodies, ligand-linked immunotoxins, tyrosine kinase inhibitors, and antisense approaches.

Recently, we have reported the design of an anti-erbB2 peptide mimetic, AHNP, derived from the structure of the CDR-H3 loop of the anti-erbB2 monoclonal antibody 4D5 and demonstrated its *in vitro* and *in vivo* activities in disabling erbB2 tyrosine kinases similar to the monoclonal antibody (14–16). We have argued that another interesting approach for disabling erbB receptor activity would be targeting protein-protein interaction surfaces. Because protein-protein interactions play a key role in various mechanisms of cellular growth and differentiation, and viral replication, inhibition of these interactions is a promising novel approach for rational drug design against a wide number of cellular and viral targets (17, 18). Synthetic peptides that disrupt protein-protein interactions have been successfully shown to act as inhibitors of HIV-1 protease (19), HIV-1 reverse transcriptase (20), herpes simplex virus ribonucleotide reductase (21), and thymidilate synthase (22). Binding of polypeptide hormones, growth factors, or cytokines to cell surface receptors activates dimerization (oligomerization) of the receptors, which leads to the signal transduction to the interior of the cell (23). Although most of the receptor inhibitors developed to date have been focused on the blockade of receptor-ligand or enzyme-substrate interactions, repression of receptor-receptor interactions that accompany oligomerization might also represent an important target for disabling receptor functioning. This approach has been recently used for the design of peptidic estrogen receptor inhibitors based on the crystal structure of the estrogen receptor dimerization interface (24).

In the present study, we have used the "dimeric interface" strategy to inhibit erbB receptor self-associations. This strat-

* This work was supported by grants from the Abramson Cancer Institute, NCI, National Institutes of Health (to M. I. G.), and from the American Cancer Society Institutional Research Grant (IRG-78-002-23) (to R. M.). The costs of publication of this article were defrayed in part by the payment of page charges. This article must therefore be hereby marked "*advertisement*" in accordance with 18 U.S.C. Section 1734 solely to indicate this fact.

‡ To whom correspondence may be addressed: Dept. of Pathology and Laboratory Medicine, University of Pennsylvania School of Medicine, 252 John Morgan Bldg., 36th and Hamilton Walk, Philadelphia, PA 19104. Tel.: 215-573-9256; Fax: 215-898-2401; E-mail: greene@reo.med.upenn.edu.

§ To whom correspondence may be addressed: Dept. of Pathology and Laboratory Medicine, University of Pennsylvania School of Medicine, 252 John Morgan Bldg., 36th and Hamilton Walk, Philadelphia, PA 19104. Tel.: 215-898-2847; Fax: 215-898-2401; E-mail: murali@xray.med.upenn.edu.

[1] The abbreviations used are: EGFR, epidermal growth factor receptor; EGF, epidermal growth factor; HIV-1, human immunodeficiency virus type 1; GST, glutathione *S*-transferase; PBS, phosphate-buffered saline; MTT, 3-(4,5-dimethylthiazol-2-yl)-2,5-diphenyltetrazolium bromide; IGF-1R, type-1 insulin-like growth factor receptor; TNF, tumor necrosis factor; IL-3, interleukin-3; HRGβ1, heregulin-β1; SPR, surface plasmon resonance; EPO, erythropoietin.

egy presumes that protein-protein interactions can be inhibited by short constrained peptides that mimic the key regions at the interface. We have recently identified distinct extracellular subdomains of erbB2 that are involved in heterodimerization with erbB1 (25). In particular, we found that the C-terminal part of subdomain IV could reduce the heteromeric signaling and transforming activities induced by EGF after associating with EGFR, suggesting a therapeutic potential for this subdomain as a target for erbB-expressing tumors. We now report a rational design of mimetic peptides derived from the extracellular subdomain IV of erbB receptors (erbB peptides) and show that these peptides can specifically bind to the receptors of the erbB family and inhibit ligand-induced receptor self-associations.

EXPERIMENTAL PROCEDURES

Peptide Synthesis and Cyclization—Linear peptides (95% purity) were ordered from the Protein Chemistry Laboratory, University of Pennsylvania. Peptide purity and identity was confirmed by reverse-phase high performance liquid chromatography and matrix-assisted laser desorption ionization mass spectrometry, using a time-of-flight mass spectrometer (MicroMass TofSpec, Micromass Inc., Beverly, MA). The peptides were cyclized by air oxidation in distilled water adjusted to pH 8.0 with $(NH_4)_2CO_3$ at 0.1 mg/ml and 4 °C. Progress of the oxidation was controlled by measuring amounts of free thiols with 5,5′-dithiobis-2-nitrobenzoic acid. Briefly, 0.4 ml of a peptide (0.1 mg/ml) and 5 μl of 5,5′-dithiobis-2-nitrobenzoic acid (20 mM) were added to 0.2 ml of 0.1 M sodium phosphate buffer, pH 8.0. Absorbance at 412 nm was measured and compared with the linear unoxidized peptides. The cyclized peptides were lyophilized and their purity analyzed by reverse-phase high performance liquid chromatography using a C18 semi-preparative column (Waters, Milford, MA). Typically, purity of higher than 95% was obtained for the cyclized peptides. Aliquots of 1 mM stock solutions have been prepared for each peptide and kept at −20 °C to be thawed prior to the binding or bioassay studies. Peptide concentrations were confirmed by UV spectrophotometry using extinction coefficients at 280 nm calculated for each peptide as described in a previous study (26).

Expression of the GST Fusion Protein of Subdomain IV of erbB2—The DNA fragment encoding the subdomain IV of erbB2 (erbB2-SbdIV) was generated by polymerase chain reaction. The upstream primer was 5′-CGCCCGGATCCTGGCCTGCCACCAGCTGTGC-3′, and the downstream primer was 5′-CGCCCGCGGCCGCCGCAGAGATGATGGAGTCAG-3′. These two primers were designed to include *Bam*HI and *Not*I restriction sites, respectively, for in-frame insertion into the *Bam*HI/*Not*I-linearized pGEX-5X-3 vector. Recombinant vector was used to infect *Escherichia coli* BL-21(DE3). 100 ml of the 2×YT medium were inoculated with 10 ml of the overnight culture and grown at 37 °C until the A_{600} of 0.4–0.5 was reached. Isopropyl-1-thio-β-D-galactopyranoside was added to the medium at the final concentration of 0.1 mM and grown for 2 h. The cells were spun down by centrifugation at 4000 × *g* for 10 min and resuspended with 5 ml of cold PBS (with dithiothreitol, phenylmethylsulfonyl fluoride, and aprotinin at the final concentrations of 5 mM, 1 mM, and 1 μg/ml, respectively). After sonication on ice, Triton X-100 was added to the final concentration of 1%, and the solution was rocked at 4 °C for 1 h and centrifuged at 10,000 × *g* for 10 min. 100 μl of glutathione Sepharose bead was then added to the supernatant. It was rocked at 4 °C for 2–4 h, centrifuged, and washed three times with PBS. 100 μl of elution buffer was added followed by rotation for 10 min at room temperature, centrifugation at 300 × *g* for 1 min, and collection of the supernatant. Elutions were repeated three times and combined.

Interaction Studies—Binding experiments were performed with the surface plasmon resonance-based biosensor instrument BIAcore 3000 (BIAcore AB, Uppsala, Sweden), at 25 °C. Recombinant purified ectodomain of erbB2 receptor was provided by Dr. Che Law, Xcyte Therapeutics, Seattle, WA. Ectodomains of erbB1 and erbB3, prepared as described in a previous study (27), were provided by Dr. Mark A. Lemmon (Department of Biochemistry and Biophysics, University of Pennsylvania School of Medicine). Immobilization of the erbB receptors in the sensor surface was performed following the standard amine coupling procedure according to manufacturer's instructions. Briefly, 35 μl of a solution containing 0.2 M *N*-ethyl-*N*′-(dimethylaminopropyl) carbodiimide and 0.05 M *N*-hydroxysuccinimide, were injected at a flow rate of 5 μl/min to activate carboxyl groups on the sensor chip surface. Receptors (40 ng/ml in 10 mM NaOAc buffer, pH 5.0) were flowed over the chip surface at a flow rate of 20 μl/min until the desired level bound protein was reached. Unreacted protein was washed out, and unreacted activated groups were blocked by the injection of 35 μl of 1 M ethanolamine at 5 μl/min. The final immobilization response of each receptor was 3500 resonance units. A reference surface was generated simultaneously under the same conditions but without receptor injection and used as a blank to correct for instrument and buffer artifacts. Peptides were injected at variable concentrations at 20 μl/min flow rate, and binding to the receptors immobilized on the chip was monitored in real-time. Each sensorgram consists of an association phase (first 240 s), reflecting binding of the injected peptide to the receptor, followed by a dissociation phase (300 s), during which the running buffer is passed over the chip and the bound peptide is being washed off the receptor surface.

MTT Assay—The MTT assay has been used for measuring cell growth as previously described (28). Briefly, T6-17 cells were seeded in 96-well plates overnight in Dulbecco's modified Eagle's medium containing 10% fetal bovine serum albumin (1000 per well). T6-17 is derived from NIH3T3 by overexpressing the human erbB2 receptor. Cells were cultured in 100 μl of fresh medium containing 1 μg/ml erbB peptides for 48 h. This incubation time was optimal for measuring inhibitory effects of different analogs. No improvements in the inhibitory activity could be achieved by increasing the incubation period. 25 μl of MTT solution (5 mg/ml in PBS) were added to each well, and after 2 h of incubation at 37 °C, 100 μl of the extraction buffer (20% w/v of SDS, 50% *N*,*N*-dimethylformamide, pH 4.7) were added. After an overnight incubation at 37 °C, the optical density at 600 nm was measured using an enzyme-linked immunosorbent assay reader.

Cell Viability and Cross-linking Analysis on 32D Cell Lines—32D cell transfectants with erbB receptors (gift from Dr. Jacalyn H. Pierce, NCI, National Institutes of Health) were grown in RPMI 1640, 10% fetal bovine serum albumin, and 5% WEHI medium (GenoQuest, interleukin-3 supplement) and respective antibiotics, *i.e.* 32D-E1 (gpt^r), 32D-E2/E3 (neo^r/gpt^r), and 32D-E2/E4 (neo^r/gpt^r) (29). The WEHI medium was withdrawn, and cells were preincubated with erbB peptides for 2 h at 37 °C before adding 10 μg/ml EGF (for 32D-E1, Collaborative Biomedical Products) or 10 μg/ml HRGβ1 (for 32D-E2/E3 or 32D E2/E4, R&D Systems) and further incubated at 37 °C for 24–48 h. The cell viability was detected with propidium iodide staining followed by flow cytometry quantification. For the cross-linking analysis, ~2×10^6 cells were suspended in RPMI 1640 medium containing 0.1% bovine serum albumin and 10 mM HEPES, and preincubated with erbB peptides for 2 h at 37 °C before adding 10 μg/ml EGF or 10 μg/ml Heregulin-β1 EGF domain and further incubated at 37 °C for 10–15 min. Cells were rinsed with PBS and incubated in 2 mM bis[sulfosuccinimidyl]suberate/PBS at 4 °C for 45 min. The cell lysate was immunoprecipitated with anti-erbB2 or anti-erbB3 antibody (Santa Cruz Biotechnology) and immunoblotted with anti-pTyr (PY20, Santa Cruz Biotechnology). To quantitate the immunoblotting analysis data, the bands corresponding to the dimeric forms of erbB receptors were scanned using the AlphaImage instrument (Alpha Innotech Corp.). At least five measurements were taken for each sample. Normalized band intensities were calculated by subtracting the background noise from each band intensity value.

Model Building—Homology modeling of erbB2-SbdIV and erbB1 ectodomain was performed with Quanta/Protein design (Molecular Simulations Inc.) on the basis of template crystal structures of laminin g1III3–5 (1KLO) for erbB2-SbdIV and insulin-like growth factor-1 receptor (1IGR) for erbB1. The sequences were aligned manually using the Sequence Viewer by matching positions of conservative cysteine residues and inserting gaps to adjust the lengths of the inter-cysteine spacings. Frameworks for the molecular models were generated by using coordinates from the template structures for manually selected matching residues of the modeled proteins. Missing coordinates for peptide segments that did not have a counterpart in the template structures were calculated by either "Regularizing Region" and "Model Side Chains" tools (for short loops) or by modeling loop conformation using a "Congen" (30, 31) program (for longer loops). The final monomeric structures were then obtained by running the CHARMm energy minimization in the Residue Topology File mode. To construct a dimeric erbB1·EGF model, the following assumptions were made based on the existing experimental evidence: erbB1·EGF complex has a 2:2 stoichiometry (32, 33); the C-terminal part of subdomain IV is a dimeric interaction site (based on our results described below); the N terminus of bound EGF is close (within about 15 Å) to Tyr-101 (subdomain I) of erbB1 (34); the C-terminal Arg-45 of bound EGF is close (within about 15 Å) to Lys-465 (subdomain III) of erbB1 (35); the N terminus of EGF bound to erbB1 is about 67 Å (from 52 to 82 Å) away from the membrane

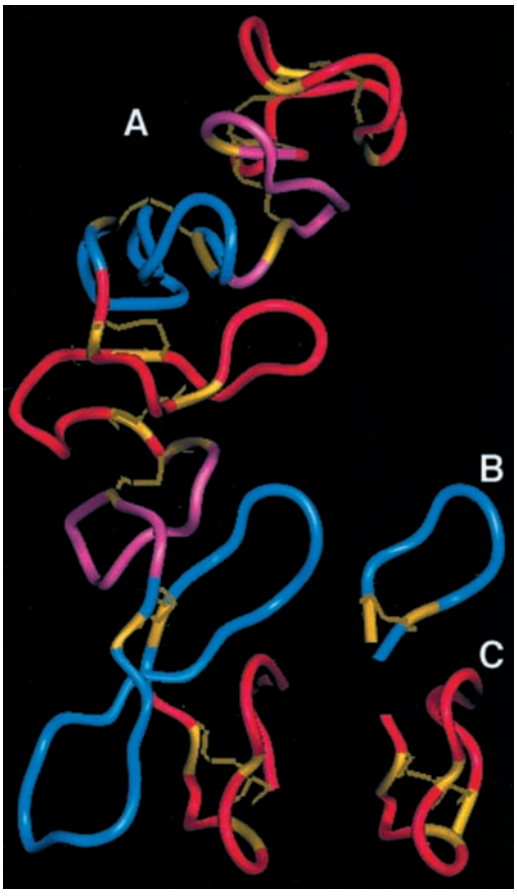

FIG. 1. **Molecular models of the extracellular subdomain IV of erbB2 (*A*) and the designed peptide mimetics B2-S22-AFA (*B*) and B2-S23-BPT (*C*).**

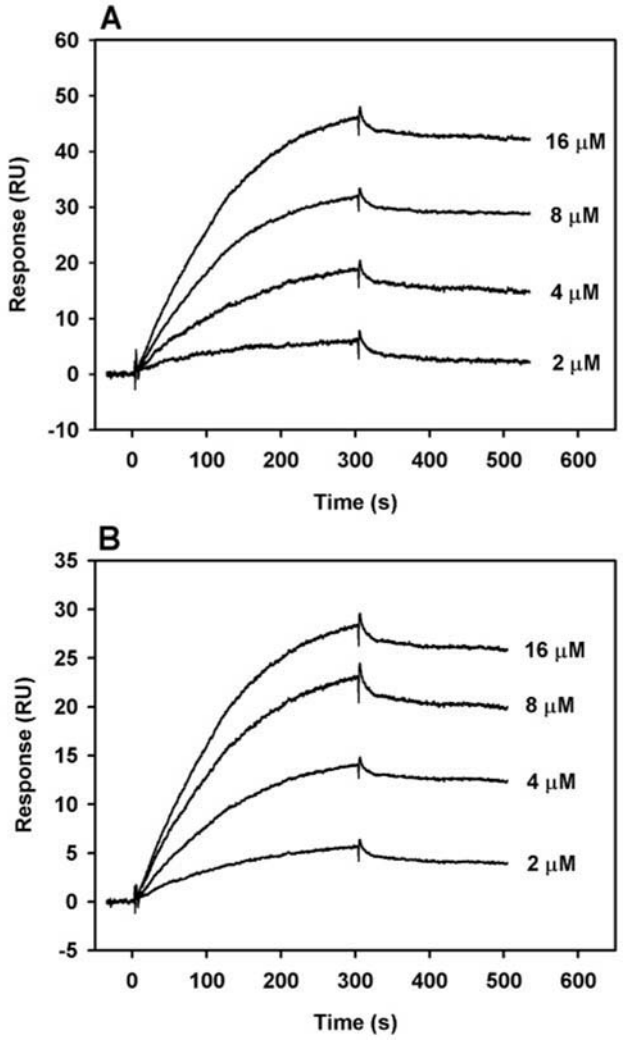

FIG. 2. **Surface plasmon resonance analysis of the interaction between the B2-S22-APE peptide and the ectodomain of erbB2 (*A*) or erbB2-SbdIV (*B*).** Dose response. The peptide was injected at four different concentrations and flowed over a surface chip with the immobilized erbB2 receptor ectodomains or erbB2-SbdIV at a flow rate of 20 μl/min.

surface (36); maximal dimensions of erbB1 are about 110 Å for the monomer and 120 Å for the dimer (32); EGF binds to the second face of subdomain III (37). Orientations of complex-forming two erbB1 and two EGF (Protein Data Bank code, 3EGF) molecules were adjusted manually to satisfy the criteria listed above based on two different models of the complex arrangement (see "Discussion"). The final dimeric models were minimized using the CHARMm energy minimization tool. These dimeric complex models have a low resolution nature and may have a degree of error in the positioning of the constituent molecules with respect to each other.

RESULTS

Molecular Modeling and Peptide Design

In the present study, we have designed constrained cyclic peptides derived from the C-terminal portion of subdomain IV that potentially mediate inter-receptor interactions between the erbB family members. The peptides were designed based on the molecular model of the subdomain IV of erbB receptors constructed by comparative modeling with the second subdomain of the type-1 insulin-like growth factor receptor (IGF-1R) (38), as well as structures of the TNF receptor and laminin that have similar disulfide bond connectivities. Most peptides mimic the S22 repeat: B1-S22-ALG (derived from erbB1), B2-S22-APE and B2-S22-AFA (derived from erbB2), B3-S22-APQ (derived from erbB3), and B4-S22-AFD (derived from erbB4). One peptide, B2-S23-BPT, was derived from the membrane-proximal S23 repeat of erbB2. A CD4 receptor-derived cyclic peptide, CD4-G, was used as a negative control. Fig. 1 shows the molecular models of the fourth subdomain of HER2 and mimetic peptides derived from the C-terminal part of this subdomain. B2-S22-AFA is a cyclic peptide that mimics part of the S22 loop, whereas B2-S23-BPT is a bicyclic peptide constrained by two disulfide bonds and actually represents a whole S23 repeat followed by the juxtamembrane amino acid residues. Molecular modeling indicates close conformational similarity between the constrained mimetic peptides and corresponding loops of the receptor.

Kinetic Binding Analysis of the erbB Peptides

The designed erbB peptides have been tested for binding to erbB receptors by means of surface plasmon resonance (BIAcore) technology. A sensorgram for binding of B2-S22-APE peptide to erbB receptors immobilized on the sensor chip is shown in Fig. 2*A*. Kinetic constants were estimated by global fitting analysis of the titration curves to the 1:1 Langmurian interaction model, which gave a k_{on} of 3.24×10^3 $M^{-1}s^{-1}$ and a k_{off} of 6.85×10^{-4} s^{-1}. The k_{off}/k_{on} ratio gave a value of 0.21 μM for the dissociation constant (K_D). Good fitting of experimental data to the calculated curves was observed, suggesting a simple pseudo-first order interaction between the peptide and the receptor. K_D values for other erbB peptides, analyzed in a similar fashion as B2-S22-APE, are presented in Table I. All erbB peptides showed binding to different erbB receptors. However, no binding could be detected to immobilized TNF receptor used as a control, indicating selectivity of erbB peptides to the

TABLE I
ErbB receptor-derived peptides
Binding to the immobilized extracellular domains of the ErbB receptors studied by surface plasmon resonance.

Peptide	Sequence	K_D(μM)			
		erbB1	erbB2	erbB3	TNFR
			μM		
B2-S23-BPT	PCPINCTHSCVDLDDKGCPAEQRASPLTSI	2.06	4.23	0.832	$>10^3$
B2-S22-APE	YCPIWKFPDEECY	0.210	1.53	1.40	$>10^3$
B1-S22-ALG	YCLVWKYADAGCY	0.449	0.371	0.288	$>10^3$
B3-S22-APQ	YCPIYKYPDVQCY	0.472	0.549	1.07	$>10^3$
B4-S22-AFD	YCPIFKYADPDCY	0.583	0.639	0.394	$>10^3$
B2-S22-AFA	YCFPDEEGACY	0.407	0.302	0.429	$>10^3$
CD4-G	FCYIGEVEDQCY	$>10^3$	$>10^3$	$>10^3$	$>10^3$

erbB receptor family. A control CD4-G peptide did not bind to any of the studied receptors. Binding specificity could also be observed for different peptides within the erbB family. Thus, erbB2-derived peptide, B2-S22-APE could bind to the erbB1 receptor much better than to erbB2 and erbB3. erbB1-derived B1-S22-ALG showed preferential binding to erbB3. On the other hand, erbB2-derived B2-S22-AFA peptide showed the best overall binding affinity to all three receptors.

To demonstrate that erbB peptides bind to SbdIV of erbB receptors, we studied interaction of the B2-S22-APE peptide with recombinantly expressed erbB2-SbdIV immobilized on the surface chip (Fig. 2*B*). The observed binding to erbB2-SbdIV had very similar kinetic constants (k_{on}, 1.62×10^3 $M^{-1}s^{-1}$; k_{off}, 3.07×10^{-3} s^{-1}) and affinity (K_D, 1.89 μM) as binding to the whole ectodomain of erbB2 (Fig. 2*A* and Table I). Likewise, binding of other erbB peptides to erbB2-Sbd IV was undistinguishable from their binding to the full-size erbB2 ectodomain (data not shown), demonstrating that subdomain IV is the binding site for all erbB peptides. Because erbB peptides are derived from subdomain IV of different erbB receptors, this fact indicates direct involvement of subdomain IV in receptor-receptor interactions between the members of erbB receptor family.

Inhibition of Receptor Self-associations

Surface Plasmon Resonance Studies—To study the effect of erbB peptides on receptor self-associations, we have developed a BIAcore assay in which the ectodomains of erbB receptors were immobilized on the surface chip and the ectodomain of erbB3 was injected at 300 nM concentrations either alone or in the presence of 5 μM HRGβ1. We noted a very limited degree of receptor-receptor interactions of these ectodomain forms in the absence of heregulin (Fig. 3, *black curves*). However, when erbB3 was preincubated with a 17-fold molar excess of HRGβ1, a strong binding to all three erbB receptors was observed (Fig. 3, *blue curves*), indicating ligand-induced homo- and heteromerization of the erbB receptor ectodomains. No increase in binding upon preincubation with heregulin was observed for the TNF receptor used as a control (data not shown). In a parallel experiment, we attempted to determine whether similar ligand-induced receptor self-associations could be observed for the erbB1 receptor injected in the presence of EGF or transforming growth factor α. However, no interaction of the injected erbB1 ectodomain (150 nM) with the immobilized receptors could be detected either in the absence or in the presence of the erbB1 ligands (5 μM), suggesting that at this erbB1 receptor concentration no significant dimerization is taking place.

Effect of the erbB peptides on heregulin-induced receptor self-associations was studied by preinjecting them at 10 μM using the "Coinject" mode of the BIAcore instrument, followed by injection of erbB3-HRGβ1 incubation mixture as described above. The inhibitory effect of B2-S22-AFA on receptor self-associations is shown in Fig. 3 (*red curves*). The peptide effectively inhibited binding of erbB3 to all three immobilized receptors. The highest degree of inhibition was observed for the erbB3-erbB2 heteromerization (82.5%) followed by erbB3-erbB1 heteromerization (78.4%) and erbB3-erbB3 homomerization (61.7%). As a control, either the running buffer or a control peptide (CD4-G) was preinjected instead of the erbB peptides and showed no effect on receptor self-associations (data not shown). Inhibition values for different erbB peptides are pre-

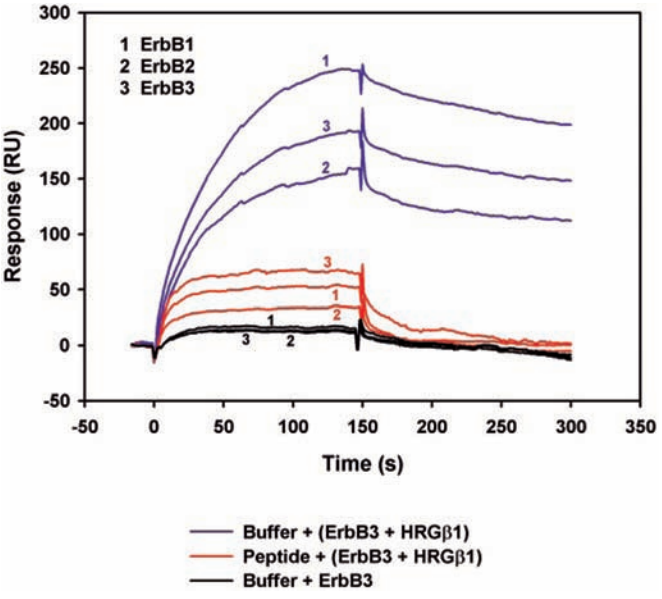

FIG. 3. **Inhibitory effect of the B2-S22-AFA peptide on heregulin-induced oligomerization of erbB receptors.** SPR analysis. erbB1, erbB2, and erbB3 were immobilized on the surface chip and 300 nM erbB3 was injected either alone (*black curves*) or in the presence of 5 μM HRGβ1 (*blue curves*). *Red curves* show binding of erbB3 to the immobilized receptors in the presence of HRGβ1 after preinjection of B2-S22-AFA at 10 μM.

TABLE II
Inhibition of ligand-induced ErbB receptor dimerization by ErbB receptor-derived peptides

	Inhibition[a]		
	erbB1	erbB2	erbB3
		%	
B2-S23-BPT	41.5	32.3	55.4
B2-S22-APE	80.3	51.1	42.7
B1-S22-ALG	65.2	71.4	75.1
B3-S22-APQ	69.0	58.1	32.4
B4-S22-AFD	60.3	54.2	72.8
B2-S22-AFA	78.4	82.5	61.7
CD4-G	2.4	−1.2	3.1

[a] Inhibitory effect of ErbB peptides (10 μM) on the binding of ErbB3 (300 nM) to the immoblilized ErbB receptors in the presence of HRGβ1 (5 μM).

sented in Table II. As expected from the data for the receptor-binding affinities, B2-S22-APE, which shows the best binding to erbB1 (Table I), is more effective in disabling interaction of erbB3 with erbB1 than with other receptors (Table II). Similarly, B1-S22-ALG with the highest erbB3-binding affinity (Table I) is the strongest inhibitor of erbB3 homomerization (Table II). B2-S22-AFA, with the strongest overall affinity to the three studied erbB receptors (Table I), is an effective inhibitor of erbB3-erbB2 and erbB3-erbB1 interactions (Table II). B2-S23-BPT, derived from the S23 repeat of erbB2, had the lowest but still significant inhibitory effect, especially on the homomerization of erbB3 (Table II) to which it binds with the highest affinity compared with other receptors (Table I).

Inhibition of Ligand-induced Dimerization of Native erbB Receptors in 32D Cell Lines—Effect of the erbB peptides on biochemically defined dimerization of native full-length erbB receptors has been studied using the 32D cell lines transfected with different erbB receptors. 32D-E1 cells were transfected with erbB1, 32D-E2/E3 with erbB2 and erbB3, and 32D-E2/E4 with erbB2 and erbB4. Fig. 4 shows the inhibitory effect of 10 μg/ml B3-S22-APQ and B2-S22-AFA on the heregulin-induced erbB2-erbB4 receptor heteromerization in the 32D-E2/E4 cells. Although B3-S22-APQ showed a significant inhibitory effect, B2-S22-AFA completely suppressed dimerization at this concentration (Fig. 4*A*). A minor inhibitory effect was observed for the CD4-G peptide used as a control. The observed inhibition of receptor dimerization by B2-S22-AFA was dose-dependent (Fig. 4*B*) with an apparent IC_{50} concentration of 0.8 μM. Similar inhibitory effects of B3-S22-APQ and B2-S22-AFA on receptor dimerization have been observed in the 32D-E2/E3 cells (data not shown).

Biological Activity of the erbB Peptides

MTT Assay—Biological activity of erbB peptides was evaluated by examining their ability to inhibit cell proliferation using standard 3-(4,5-dimethylthiazol-2-yl)-2,5-diphenyltetrazolium bromide (MTT) assays (28). HER2-expressing transformed tumor cells (T6-17) were used for this purpose (14). In MTT assays, the peptides inhibited the growth of T6-17 cells, an erbB2-overexpressing transformed cell line, dose-dependently at concentrations ranging from 0.01 to 10 μg/ml. The biological activity of erbB peptides at the optimal concentration of 1 μg/ml is shown in Fig. 5. Each value represents an average of at least four samples. All peptides displayed inhibitory effects on cell growth. B2-S22-AFA, which has the highest erbB2 receptor-binding affinity (Table I), was also the most active peptide in the MTT assay (Fig. 5).

To find out whether the observed biological activities of erbB2 peptides against T6-17 cells correlate with their receptor binding properties or their inhibitory activity on receptor-receptor interactions, we have plotted the binding data shown in Tables I and II against the MTT assay data shown in Fig. 5 for all studied peptides (Fig. 6). Although there is a strong correlation (r = 0.92) between the biological activity and binding affinity to erbB2, correlation with binding affinities to other erbB receptors (erbB1 and erbB3) was insignificant (r = 0.21 and 0.44, respectively, Fig. 6*A*). Similarly, a strong correlation (r = 0.91) has been observed between the cell-suppressing activity and inhibitory activity against erbB3-erbB2 interactions, but not against erbB3-erbB1 (r = 0.29) or erbB3-erbB3 (r = 0.17) interactions (Fig. 6*B*).

Effect on the Viability of 32D Cell Lines—Inhibitory effects of the erbB peptides on cells overexpressing erbB receptors has been tested using the 32D cell lines. Transfection of 32D cells with erbB receptors created the transfectants capable of growing in a medium containing either EGF (32D-E1), HRGβ1 (32D-E2/E3 and 32D-E2/E4), or IL-3 (supplement WEHI medium, all three cell lines) (39). Fig. 7*A* shows the effect of different erbB peptides on the viability of the 32D transfectants grown in the erbB ligand medium. The strongest inhibitory effect was observed for the 32D-E1 cells (grown in the EGF medium). The effect on the 32D-E2/E3 and 32D-E2/E4 cells (grown in the HRGβ1 medium) was less pronounced but also significant (Fig. 7*A*). However, when the same cell lines were grown in the IL-3 supplement WEHI medium, no significant effect on cell viability could be detected for any of the studied peptides (Fig. 7*B*), confirming that the observed inhibition of cell survival by the erbB peptides is mediated by their specific effect on the erbB receptor signaling but not on IL-3-related signaling.

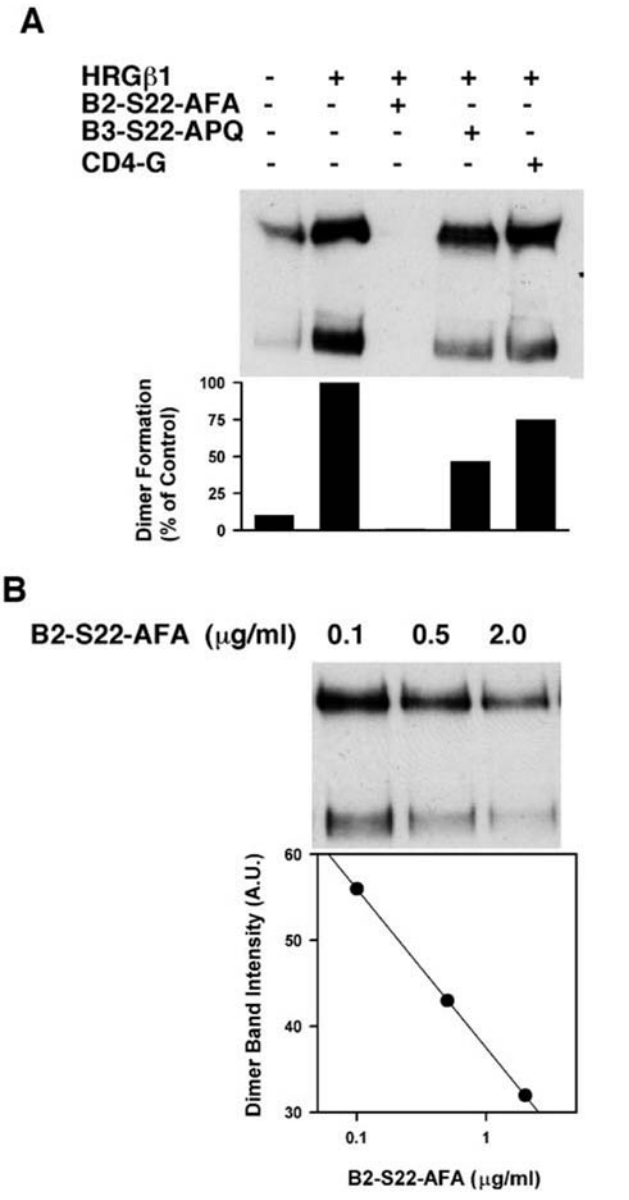

FIG. 4. **Inhibitory effect of the B2-S22-AFA and B3-S22-APQ peptides on heregulin activation and dimerization of erbB receptors.** *A*, 32D-E2/E4 cells were incubated in the absence (−) or presence (+) of 10 μg/ml HRGβ1 and 10 μg/ml erbB peptides and analyzed by chemical cross-linking and immunoblotting experiments as described under "Experimental Procedures." The *inset* shows intensities of bands corresponding to the dimeric receptor forms quantitated as described under "Experimental Procedures." Average values of at least five quantitations are shown. Standard deviations did not exceed 5% for all samples. *B*, dose response of the inhibitory effect by the B2-S22-AFA peptide. The *inset* shows the same dose response as a plot of dimer band intensities *versus* B2-S22-AFA concentration.

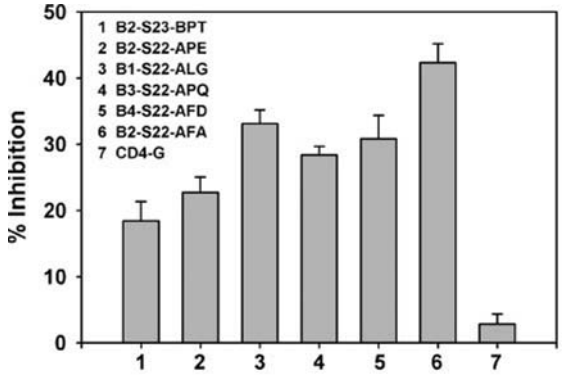

FIG. 5. **Inhibitory activity of the erbB peptides against the growth of T6-17 cells studied in an MTT assay.**

DISCUSSION

Here we have shown that mimetic constrained peptides derived from the extracellular domain of different erbB receptors can specifically bind to the receptors of the erbB family and inhibit ligand-induced receptor self-associations. The inhibitory effects on receptor-receptor interactions have been demonstrated for both the ectodomains in SPR experiments (Fig. 3) and for the native full-length receptors in 32D cell lines (Fig. 4). The observed blockade of receptor-receptor interactions resulted in the suppression of growth in cells overexpressing erbB receptors (Figs. 5 and 7).

Although ligand-induced homo- and heteromerization of the full-length native erbB receptors has been established and well documented, experimental data on self-associations of the extracellular domains of these receptors are somewhat contradictory. In analytical ultracentrifugation and MALLS studies, ligand-induced homodimerization has been demonstrated for erbB1 and erbB4 (27). However, homo-oligomerization was not observed for the erbB3 receptor, and the only erbB receptor combinations that produced heterodimers in the presence of hrgβ1 were erbB2-erbB4 and to a smaller extent erbB2-erbB3. In contrast, both erbB3 homodimerization and erbB3-erbB2 heterodimerization have been reported for the ectodomains, but these effects could only be observed when ectodomains of the receptors were anchored to the membrane (40). Landgraf and Eisenberg (41) have reported ligand-independent self-association of erbB3 ectodomains that could be disrupted by HRGβ1. Although both monomeric and oligomeric forms of erbB3 were detected in the presence of hrgβ1 by size-exclusion chromatography, addition of the ligand produced a shift toward a low molecular mass species.

Our SPR data indicate that the ectodomain of erbB3 preincubated with hrgβ1 can interact with ligand-free forms of erbB1, erbB2, and erbB3 ectodomains immobilized on the surface chip (Fig. 3). A possible reason for the discrepancies between our results and those previously reported (41) could be a different procedure used for the immobilization of the erbB receptors. We used a standard amino-coupling procedure that results in a heterogeneous population of the receptor molecules in terms of their site of attachment to the surface chip and their relative spatial orientations. In contrast, in a previous study (41), an anti-erbB3 antibody was immobilized first and used as an anchor for the immobilization of erbB3, resulting in a homogenous erbB3 population. It is possible that, upon binding of erbb3 to the antibody, the site on the receptor surface involved in the ligand-induced receptor-receptor interaction has been blocked by the antibody molecule so that no ligand-induced oligomerization could be observed in the presence of heregulin. In our experiments, we also observed some limited ligand-independent oligomerization of erbB3 with the immobilized erbB receptors (Fig. 3, *black curves*). However, addition of heregulin led to a much stronger ligand-induced oligomerization (Fig. 3, *blue curves*). If heregulin induced dissociation of the ligand-independent oligomers (41), then according to our data, this dissociation must be accompanied by a rearrangement of the ligand-free complexes into new ligand-induced oligomers with different relative orientations of the monomeric receptor molecules and new receptor-receptor contact sites. These new sites must have been blocked under conditions used previously (41) but are exposed and functional in our experimental protocol. The ligand-activated rearrangement of the erbB receptors could thus be similar to the one proposed for the EPO receptor upon addition of EPO (42), where the unliganded EPO receptor exists as an inactive dimer but undergoes an activating conformational change upon binding of EPO.

erbB peptides described in this study represent constrained mimics of the loops or repeats present in the subdomain IV of the erbB receptors and, based on our modeling studies, show a high degree of structural similarity with the template receptor regions (Fig. 1). Therefore, there is a strong probability that the interactions observed for the erbB peptides can also be displayed by the corresponding sites of the native erbB receptors and play a certain role in their metabolic activity. In this regard, information obtained for the B2-S23-BTE peptide is especially valuable, because, unlike other designed erbB peptides, it does not mimic a single loop but rather represents a C-terminal membrane-proximal portion of the erbB2 ectodomain. Thus, because the C-terminal portion of erbB2 (B2-S23-BPT) can bind to all three studied erbB receptors (Table I), this property is also likely to be expected from the full-length native erbB2 receptor. The fact that the designed cyclic erbB peptides are not specific to any particular erbB receptor but are highly specific to the erbB family (Table I), suggests that the C-terminal part of subdomain IV is a receptor-receptor interaction site shared by all erbB receptors. Because all erbB peptides could bind to the parental receptor and to other erbB receptors (Table I), these sites can participate in both homo- and heteroreceptor self-associations.

A variety of possible ways in which receptors can self-associate has been demonstrated crystallographically for the EPO (43, 44) and TNF receptors (45–47), including the formation of ligand-free parallel and anti-parallel dimers in addition to the traditional dimeric receptor-ligand complex. Each of the observed inter-receptor binding modes might play an important role at different stages of receptor functioning. Our recent experimental data on erbB1-erbB2 interactions, showing that numerous separate subdomains of erbB2 can bind to the full-length erbB1 (25), further suggest that oligomerization of cell surface receptors, comprising the whole network of individual inter-receptor interactions involved in signaling, is a complex multistep process that cannot be limited to a simple formation of a dimeric receptor-ligand complex. Thus, erbB (48, 49) and other receptors (43, 50–54) may pre-exist as ligand-free dimeric complexes that form high affinity ligand binding sites and can rearrange (or twist) upon ligand binding to form efficient signaling complexes (48). Ligand-bound receptor forms could further interact with each other or with ligand-free forms (46). In addition, ligand-independent interaction of receptors with their soluble isoforms or decoy receptors has been shown for erbB and other receptors (55–57). Each of these bound conformations probably involves different types of inter-receptor interactions and, therefore, uses different binding epitopes on the receptor surface, which come into play under certain circumstances to ensure the proper receptor functioning. The presence of multiple epitopes spread over the receptor surface,

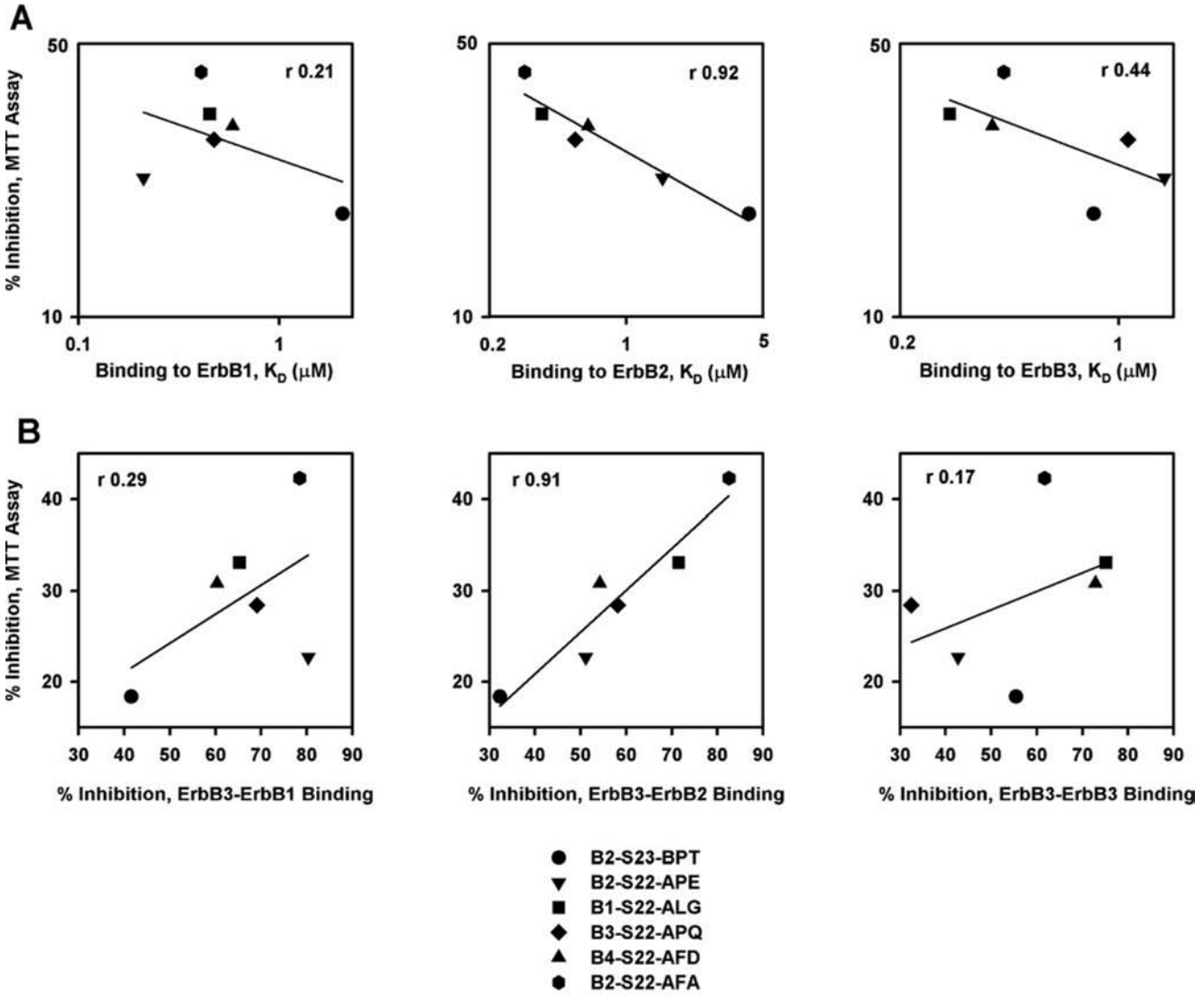

FIG. 6. **Correlation between receptor binding properties of the erbB peptides and their biological activity against erbB2-overexpressing T6-17 cells.** Plots show correlation between peptides' activities in MTT assays and (*A*) their receptor-binding affinities or (*B*) their inhibitory activity against erbB receptor oligomerization.

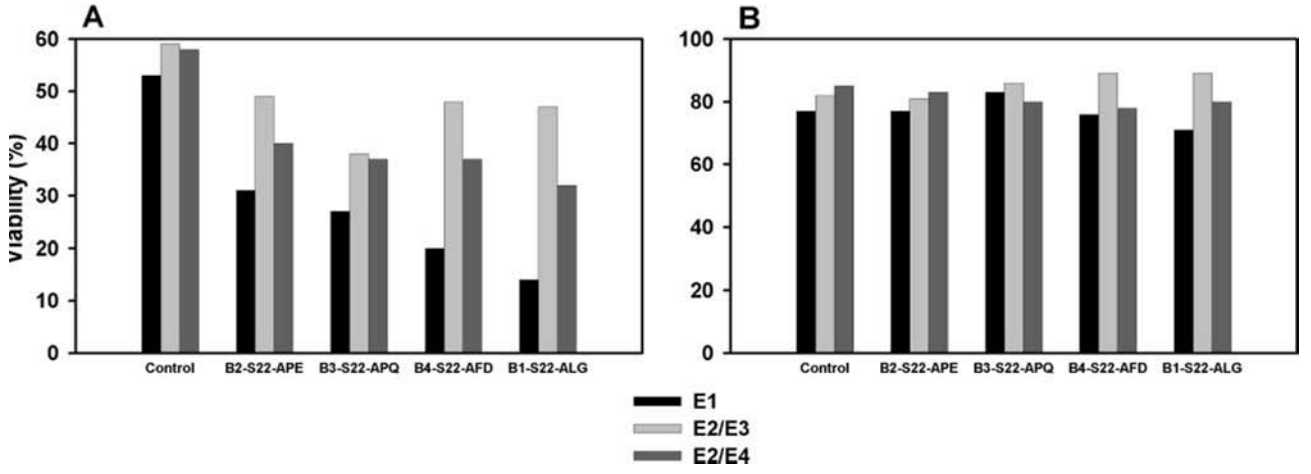

FIG. 7. **Inhibitory effect of the erbB peptides on cell survival of the 32D cell transfectants.** 32D cell transfectants were grown in either the erbB ligand medium (*A*) or the IL-3 supplement (WEHI) medium (*B*), and cell viability was determined as described under "Experimental Procedures." In all experiments, the standard error did not exceed 10%.

each playing a certain role at different points of signaling, could explain why many of the studied epitope-containing erbB2 subdomains (25) and subdomain IV-derived mimetic peptides described herein could interact with the erbB receptors. With no conformational constraints imposed by the neighboring receptor subdomains, which in native receptors might limit the

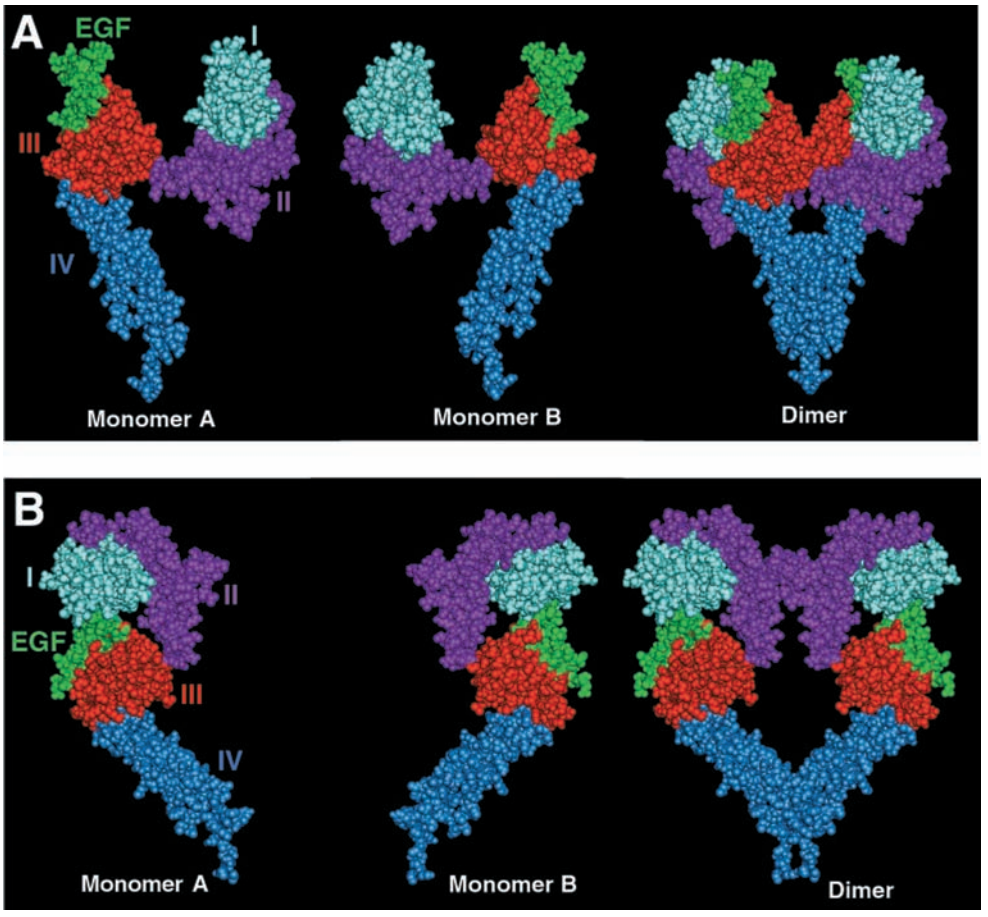

FIG. 8. **Molecular modeling of erbB1 homodimerization.** Possible arrangement of the erbB1·EGF (2:2) complex according to model 1 (EGF cross-links two erbB1 monomers, *A*) and model 2 (EGF binds to one erbB1 monomer, *B*).

number of possible interactions at any given point in time, thus preventing uncontrolled signaling, the isolated subdomains or mimetic peptides could effectively bind to a receptor regardless of its current conformational state.

Because of the mentioned complexity of the receptor oligomerization mechanism, interpretation of the experimentally observed inter-receptor interactions may not be straightforward. The interactions observed in our SPR studies (Fig. 3) might lead to the formation of a dimeric receptor-ligand complex. Fig. 8 shows molecular models for possible arrangement of the erbB1·EGF complex. Based on the existing experimental evidence, this complex is likely to have a 2:2 receptor-ligand stoichiometry with EGF bound to both subdomains I and II (32–35). There are two possible ways in which EGF can interact with subdomains I and III within the complex. It can either cross-link subdomains I and III of two different EGFR monomers (model 1, Fig. 8*A*) or it can bind to subdomains I and III of the same EGFR monomer (model 2, Fig. 8*B*). In both models (Fig. 8), subdomains I–III of the monomeric erbB1 were built by comparative modeling with the homologous subdomains I–III of the type-1 insulin-like growth factor receptor (IGF-1R) (38). The fourth subdomain of erbB1 has been constructed as described above (Fig. 1). In model 1 of the dimeric complex (Fig. 8*A*), we assumed same relative orientation of erbB1 monomers as that proposed for the homologous insulin receptor based on the electron microscopy studies (58). The insulin receptor is a covalently linked homo-dimer with a U-shaped arrangement of the first three extracellular subdomains, in which subdomain I of one monomer is located next to subdomain III of the other one. According to model 1 of the EGFR homodimer (Fig. 8*A*), EGF molecules are in contact with subdomains I and III of different monomers. Subdomain IV is membrane-proximal and contains the inter-monomer disulfide bonds. Although subdomain IV of erbB1 is not homologous to the subdomain IV of the insulin receptor, we can assume that in erbB receptors, subdomains IV of the two monomers are also located next to each other potentially making non-covalent contacts in their C-terminal region (Fig. 8*A*). In model 2 (Fig. 8*B*), relative orientations of the N-terminal (subdomains I and II) and the C-terminal (subdomains III and IV) halves of EGFR should differ significantly from the arrangement of IGF-1R. An rotation of ~90 degree of subdomains I and II toward subdomains III and IV around a hinge region (located between subdomains II and III) would be necessary to allow one EGF molecule to be in contact with subdomains I and III of the same EGFR monomer. In both proposed models, the C-terminal part of subdomain IV is one of the inter-receptor contact sites. These contacts may be necessary for the formation of a functional dimer. Blocking them with the mimics of their counterparts in the dimeric complex results in the inhibitory activity displayed by the erbB peptides. Although erbB peptides should bind to the C-terminal part of subdomain IV, according to the molecular models presented in Fig. 8, they are unlikely to bind precisely to the corresponding sites that contain their own sequences on the receptor surface. If that were the case, peptide self-associations could be taking place. However, our size-exclusion chromatography analysis of erbB peptides did not reveal any dimeric or oligomeric peptide forms (data not shown).

The observed receptor-receptor interactions (Fig. 3) may as well represent a higher-order oligomerization event in which ligand-induced dimers formed in the receptor-ligand incubation mixture bind to the ligand-free receptors immobilized on

the surface chip, thus creating an extended receptor complex, as it has been proposed for the TNF receptor (46). This complex extension could be a necessary step in a process eventually leading to the receptor clustering, a common phenomenon that has been observed for the erbB (59–62) and other cell surface receptors (63–71) in various *in vitro* and *in vivo* studies.

Regardless of the exact mechanism, the observed inter-receptor interactions involving the C-terminal portion of subdomain IV are obviously playing an important role in the receptor functioning. Indeed, specific inhibition of these interactions by the erbB peptides resulted in a dramatic suppression of the cell growth (Figs. 5 and 8). The specificity of the biological effects displayed by erbB peptides has been demonstrated in different erbB receptor-expressing cell lines. Because T6-17 cells are characterized by overexpressed levels of erbB2 receptor but negligible levels of other erbB receptors, erbB2 binding properties of erbB peptides are likely to be more important determinants of their inhibitory effects on T6-17 cell growth than their erbB1 or erbB3 binding properties. Thus significant correlation between peptides binding to erbB2 (Fig. 6*A*) and their inhibition of erbB3-erbB2 binding (Fig. 6*B*) and inhibitory activity against erbB2-overexpressing T6-17 cells in the MTT assay strongly suggest that, in these cells, the observed biological activities of erbB peptides are mediated by their binding to the erbB2 receptor and by blocking receptor-receptor interactions that involve erbB2, most likely erbB2 homomerization. This conclusion is further supported by the fact that peptide-binding affinities for other erbB receptors (erbB1 and erbB3), which are not significantly expressed in T6-17 cells, have no effect on their biological activity (Fig. 6*A*). Moreover, the ability of peptides to block receptor-receptor associations that don't involve erbB2 (such as erbB3-erbB1 and erbB3-erbB3 interactions) is also unimportant for their activity in the MTT assay (Fig. 6*B*). erbB peptide-induced inhibition of cell growth in 32D cells transfected with erbB receptors has also been shown to be specifically mediated by the erbB receptor pathway. Indeed, strong inhibition of cell growth has been observed only when the cells were grown in the erbB ligand medium (Fig. 7*A*). In contrast, no inhibition occurred via an erbB receptor-independent pathway when the cells were grown in the IL-3 supplement (WEHI) medium (Fig. 7*B*).

In conclusion, we have shown that erbB receptor signaling can be inhibited by rationally designed interface peptide mimetics derived from the subdomain IV of erbB receptor ectodomains. The mimetics specifically bind to the receptors of the erbB family and block inter-receptor interactions, which leads to the growth inhibition of HER2-overexpressing cells *in vitro*. Because all four erbB receptors represent a therapeutic target, peptide mimetics that selectively bind to this receptor family and disable their activity could have an advantage over drugs that are specific to a single member of the erbB family. The study also demonstrates the importance of the C-terminal part of subdomain IV for receptor-receptor interactions involved in signaling by erbB family members.

Acknowledgments—We thank the University of Pennsylvania Cancer Center and American Cancer Society for the grant support, the Biosensor/Interaction Analysis and Structural Biology Cores Group, Department of Medicine, University of Pennsylvania for assistance with BIAcore binding studies, and the Protein Chemistry Laboratory, University of Pennsylvania, for peptide synthesis and purification.

REFERENCES

1. Dougall, W. C., Qian, X., Peterson, N. C., Miller, M. J., Samanta, A., and Greene, M. I. (1994) *Oncogene* **9,** 2109–2123
2. Hynes, N. E., and Stern, D. F. (1994) *Biochim. Biophys. Acta* **1198,** 165–184
3. Reese, D. M., and Slamon, D. J. (1997) *Stem Cells* **15,** 1–8
4. Alroy, I., and Yarden, Y. (1997) *FEBS Lett.* **410,** 83–86
5. Drebin, J. A., Link, V. C., and Greene, M. I. (1988) *Oncogene* **2,** 273–277
6. O'Rourke, D. M., and Greene, M. I. (1998) *Immunol. Res.* **17,** 179–189
7. Murali, R., and Greene, M. I. (1998) *Immunol. Res.* **17,** 163–169
8. O'Rourke, D. M., Kao, G. D., Singh, N., Park, B. W., Muschel, R. J., Wu, C. J., and Greene, M. I. (1998) *Proc. Natl. Acad. Sci. U. S. A.* **95,** 10842–10847
9. O'Rourke, D. M., Nute, E. J., Davis, J. G., Wu, C., Lee, A., Murali, R., Zhang, H. T., Qian, X., Kao, C. C., and Greene, M. I. (1998) *Oncogene* **16,** 1197–1207
10. Wels, W., Harwerth, I. M., Hynes, N. E., and Groner, B. (1992) *J. Steroid Biochem. Mol. Biol.* **43,** 1–7
11. Zhang, H., Wang, Q., Montone, K. T., Peavey, J. E., Drebin, J. A., Greene, M. I., and Murali, R. (1999) *Exp. Mol. Pathol.* **67,** 15–25
12. Wels, W., Harwerth, I. M., Mueller, M., Groner, B., and Hynes, N. E. (1992) *Cancer Res.* **52,** 6310–6317
13. Xu, F. J., Boyer, C. M., Bae, D. S., Wu, S., Greenwald, M., O'Briant, K., Yu, Y. H., Mills, G. B., and Bast, R. C., Jr. (1994) *Int. J. Cancer* **59,** 242–247
14. Park, B. W., Zhang, H. T., Wu, C., Berezov, A., Zhang, X., Dua, R., Wang, Q., Kao, G., O'Rourke, D. M., Greene, M. I., and Murali, R. (2000) *Nat. Biotechnol.* **18,** 194–198
15. Berezov, A., Zhang, H.-T., Greene, M. I., and Murali, R. (2001) *BIAjournal* **8,** 4–7
16. Berezov, A., Zhang, H.-T., Greene, M. I., and Murali, R. (2001) *J. Med. Chem.* **44,** 2565–2574
17. Zutshi, R., Brickner, M., and Chmielewski, J. (1998) *Curr. Opin. Chem. Biol.* **2,** 62–66
18. Peczuh, M. W., and Hamilton, A. D. (2000) *Chem. Rev.* **100,** 2479–2494
19. Schramm, H. J., Boetzel, J., Buttner, J., Fritsche, E., Gohring, W., Jaeger, E., Konig, S., Thumfart, O., Wenger, T., Nagel, N. E., and Schramm, W. (1996) *Antiviral Res.* **30,** 155–170
20. Divita, G., Restle, T., Goody, R. S., Chermann, J. C., and Baillon, J. G. (1994) *J. Biol. Chem.* **269,** 13080–13083
21. Dutia, B. M., Frame, M. C., Subak-Sharpe, J. H., Clark, W. N., and Marsden, H. S. (1986) *Nature* **321,** 439–441
22. Prasanna, V., Bhattacharjya, S., and Balaram, P. (1998) *Biochemistry* **37,** 6883–6893
23. Heldin, C. H. (1995) *Cell* **80,** 213–223
24. Yudt, M. R., and Koide, S. (2001) *Steroids* **66,** 549–558
25. Kumagai, T., Davis, J. G., Horie, T., O'Rourke, D. M., and Greene, M. I. (2001) *Proc. Natl. Acad. Sci. U. S. A.* **98,** 5526–5531
26. Gill, S. C., and von Hippel, P. H. (1989) *Anal. Biochem.* **182,** 319–326
27. Ferguson, K. M., Darling, P. J., Mohan, M. J., Macatee, T. L., and Lemmon, M. A. (2000) *EMBO J.* **19,** 4632–4643
28. Hansen, M. B., Nielsen, S. E., and Berg, K. (1989) *J. Immunol. Methods* **119,** 203–210
29. Alimandi, M., Wang, L. M., Bottaro, D., Lee, C. C., Kuo, A., Frankel, M., Fedi, P., Tang, C., Lippman, M., and Pierce, J. H. (1997) *EMBO J.* **16,** 5608–5617
30. Li, H., Tejero, R., Monleon, D., Bassolino-Klimas, D., Abate-Shen, C., Bruccoleri, R. E., and Montelione, G. T. (1997) *Protein Sci.* **6,** 956–970
31. Tejero, R., Bassolino-Klimas, D., Bruccoleri, R. E., and Montelione, G. T. (1996) *Protein Sci.* **5,** 578–592
32. Lemmon, M. A., Bu, Z., Ladbury, J. E., Zhou, M., Pinchasi, D., Lax, I., Engelman, D. M., and Schlessinger, J. (1997) *EMBO J.* **16,** 281–294
33. Odaka, M., Kohda, D., Lax, I., Schlessinger, J., and Inagaki, F. (1997) *J. Biochem. (Tokyo)* **122,** 116–121
34. Woltjer, R. L., Lukas, T. J., and Staros, J. V. (1992) *Proc. Natl. Acad. Sci. U. S. A.* **89,** 7801–7805
35. Summerfield, A. E., Hudnall, A. K., Lukas, T. J., Guyer, C. A., and Staros, J. V. (1996) *J. Biol. Chem.* **271,** 19656–19659
36. Carraway, K. L., 3rd, Koland, J. G., and Cerione, R. A. (1990) *Biochemistry* **29,** 8741–8747
37. Jorissen, R. N., Epa, V. C., Treutlein, H. R., Garrett, T. P., Ward, C. W., and Burgess, A. W. (2000) *Protein Sci.* **9,** 310–324
38. Garrett, T. P., McKern, N. M., Lou, M., Frenkel, M. J., Bentley, J. D., Lovrecz, G. O., Elleman, T. C., Cosgrove, L. J., and Ward, C. W. (1998) *Nature* **394,** 395–399
39. Wang, L. M., Kuo, A., Alimandi, M., Veri, M. C., Lee, C. C., Kapoor, V., Ellmore, N., Chen, X. H., and Pierce, J. H. (1998) *Proc. Natl. Acad. Sci. U. S. A.* **95,** 6809–6814
40. Tzahar, E., Pinkas-Kramarski, R., Moyer, J. D., Klapper, L. N., Alroy, I., Levkowitz, G., Shelly, M., Henis, S., Eisenstein, M., Ratzkin, B. J., Sela, M., Andrews, G. C., and Yarden, Y. (1997) *EMBO J.* **16,** 4938–4950
41. Landgraf, R., and Eisenberg, D. (2000) *Biochemistry* **39,** 8503–8511
42. Remy, I., Wilson, I. A., and Michnick, S. W. (1999) *Science* **283,** 990–993
43. Livnah, O., Stura, E. A., Middleton, S. A., Johnson, D. L., Jolliffe, L. K., and Wilson, I. A. (1999) *Science* **283,** 987–990
44. Syed, R. S., Reid, S. W., Li, C., Cheetham, J. C., Aoki, K. H., Liu, B., Zhan, H., Osslund, T. D., Chirino, A. J., Zhang, J., Finer-Moore, J., Elliott, S., Sitney, K., Katz, B. A., Matthews, D. J., Wendoloski, J. J., Egrie, J., and Stroud, R. M. (1998) *Nature* **395,** 511–516
45. Banner, D. W., D'Arcy, A., Janes, W., Gentz, R., Schoenfeld, H. J., Broger, C., Loetscher, H., and Lesslauer, W. (1993) *Cell* **73,** 431–445
46. Naismith, J. H., Brandhuber, B. J., Devine, T. Q., and Sprang, S. R. (1996) *J. Mol. Recognit.* **9,** 113–117
47. Naismith, J. H., Devine, T. Q., Kohno, T., and Sprang, S. R. (1996) *Structure* **4,** 1251–1262
48. Gadella, T. W., Jr., and Jovin, T. M. (1995) *J. Cell Biol.* **129,** 1543–1558
49. Sako, Y., Minoghchi, S., and Yanagida, T. (2000) *Nat. Cell Biol.* **2,** 168–172
50. Chan, F. K., Chun, H. J., Zheng, L., Siegel, R. M., Bui, K. L., and Lenardo, M. J. (2000) *Science* **288,** 2351–2354
51. Siegel, R. M., Frederiksen, J. K., Zacharias, D. A., Chan, F. K., Johnson, M., Lynch, D., Tsien, R. Y., and Lenardo, M. J. (2000) *Science* **288,** 2354–2357
52. Crottet, P., Peitsch, M. C., Servis, C., and Corthesy, B. (1999) *J. Biol. Chem.* **274,** 31445–31455
53. Gilboa, L., Nohe, A., Geissendorfer, T., Sebald, W., Henis, Y. I., and Knaus, P. (2000) *Mol. Biol. Cell* **11,** 1023–1035

54. McVey, M., Ramsay, D., Kellett, E., Rees, S., Wilson, S., Pope, A. J., and Milligan, G. (2001) *J. Biol. Chem.* **276,** 14092–14099
55. Doherty, J. K., Bond, C., Jardim, A., Adelman, J. P., and Clinton, G. M. (1999) *Proc. Natl. Acad. Sci. U. S. A.* **96,** 10869–10874
56. Prevost, J. M., Farrell, P. J., Iatrou, K., and Brown, C. B. (2000) *Cytokine* **12,** 187–197
57. Ashkenazi, A., and Dixit, V. M. (1998) *Science* **281,** 1305–1308
58. Tulloch, P. A., Lawrence, L. J., McKern, N. M., Robinson, C. P., Bentley, J. D., Cosgrove, L., Ivancic, N., Lovrecz, G. O., Siddle, K., and Ward, C. W. (1999) *J. Struct. Biol.* **125,** 11–18
59. Crouch, M. F., Davy, D. A., Willard, F. S., and Berven, L. A. (2000) *Immunol. Cell Biol.* **78,** 408–414
60. Crouch, M. F., Davy, D. A., Willard, F. S., and Berven, L. A. (2001) *J. Cell Biol.* **152,** 263–273
61. Nagy, P., Jenei, A., Kirsch, A. K., Szollosi, J., Damjanovich, S., and Jovin, T. M. (1999) *J. Cell Sci.* **112,** 1733–1741
62. van Belzen, N., Rijken, P. J., Hage, W. J., de Laat, S. W., Verkleij, A. J., and Boonstra, J. (1988) *J. Cell. Physiol.* **134,** 413–420
63. Chen, L., Wang, H., Vicini, S., and Olsen, R. W. (2000) *Proc. Natl. Acad. Sci. U. S. A.* **97,** 11557–11562
64. Cochran, J. R., Aivazian, D., Cameron, T. O., and Stern, L. J. (2001) *Trends Biochem. Sci.* **26,** 304–310
65. Hirai, H. (2001) *Neurosci. Res.* **39,** 261–267
66. Kamboj, S., and Huganir, R. L. (1998) *Curr. Biol.* **8,** R719–R721
67. Krawczyk, C., and Penninger, J. M. (2001) *Trends Cell Biol.* **11,** 212–220
68. Krawczyk, C., and Penninger, J. M. (2001) *J. Leukoc. Biol.* **69,** 317–330
69. Kwong, E., and Gu, Q. (2000) *Neuroreport* **11,** 2703–2706
70. Mohamed, A. S., Rivas-Plata, K. A., Kraas, J. R., Saleh, S. M., and Swope, S. L. (2001) *J. Neurosci.* **21,** 3806–3818
71. Sitrin, R. G., Pan, P. M., Harper, H. A., Todd, R. F., 3rd, Harsh, D. M., and Blackwood, R. A. (2000) *J. Immunol.* **165,** 3341–3349